APRIL 30, 2021

TRIBOLOGY TEST BED TECHNICAL REPORT

NiWC3B Cermet, Chloride Salts

EVAN OGREN
UNIVERSITY OF WISCONSIN - MADISON
Rev: Dr. Mark Anderson

Contents

Test Matrix and Overview

To study the material validity relating to wear and erosion of Nickel Tungsten Carbide (NiWC3b) in chloride salts ($MgCl_2$-KCl-NaCl), a 500-hour tribology test was conducted. The test was comprised of three NiWC3b journal bearings, three SS316 HVOF NiWC3b-coated shaft sleeves, and five cylindrical NiWC3b pin specimens fully submersed in salt at 720°C. Table 1 gives a summary of the test including test conditions and information regarding the samples.

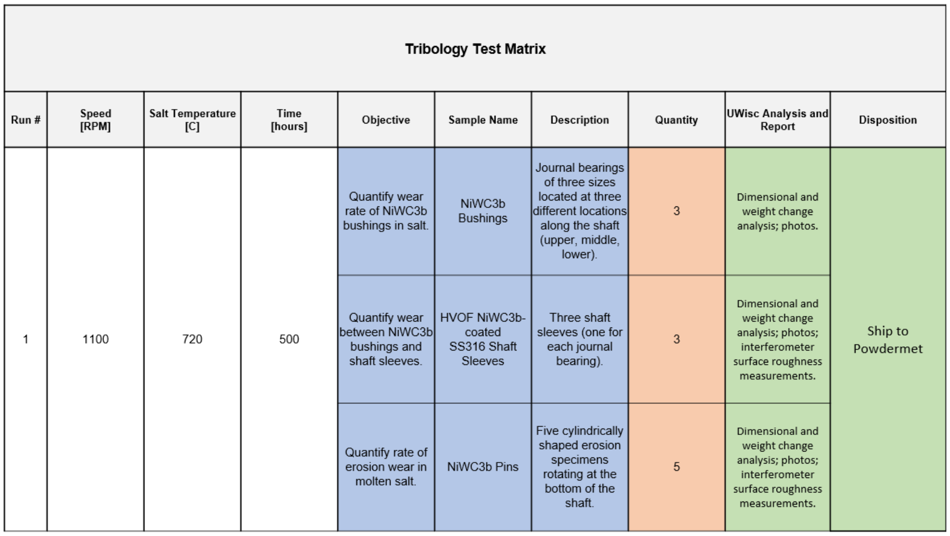

Tribology Test Matrix

Run #	Speed [RPM]	Salt Temperature [C]	Time [hours]	Objective	Sample Name	Description	Quantity	UWisc Analysis and Report	Disposition
1	1100	720	500	Quantify wear rate of NiWC3b bushings in salt.	NiWC3b Bushings	Journal bearings of three sizes located at three different locations along the shaft (upper, middle, lower).	3	Dimensional and weight change analysis; photos.	Ship to Powdermet
				Quantify wear between NiWC3b bushings and shaft sleeves.	HVOF NiWC3b-coated SS316 Shaft Sleeves	Three shaft sleeves (one for each journal bearing).	3	Dimensional and weight change analysis; photos; interferometer surface roughness measurements.	
				Quantify rate of erosion wear in molten salt.	NiWC3b Pins	Five cylindrically shaped erosion specimens rotating at the bottom of the shaft.	5	Dimensional and weight change analysis; photos; interferometer surface roughness measurements.	

Table 1. Tribology test bed test matrix.

Salt preparation: ICL Salt

The tribology test bed required approximately 70 kg of chloride salt ($MgCl_2$-KCl-NaCl) composed of a mixture of two salts, Anhydrous Carnalite (AC) salt (ICL Industrial Products), and SPK Halite (NaCl, Albermale). 65 g of SPK halite were added per 1 kg of AC salt, and solid Magnesium was added at 2.5 g of Magnesium per 1 kg of AC salt for a target composition of wt. 45.98% $MgCl_2$, wt. 38.91% KCl, and wt. 15.11 % NaCl. The salt was prepared following the NREL purification procedure [1], modified to accommodate the 70 kg of salt needed.

For the purification, a vessel of Ni201 NPS 12'' was used (The Ni201 was corroded heavily by the salt at high temperature and thus is not recommended. C-276 worked well as a purification vessel material for a subsequent purification). A quantity of 85.4 kg of salt (80 kg AC salt, 5.2 kg SPK halite, and 0.2 kg of Mg) was purified with approximately 70 kg for use in the tribology test rig. The purification took place over the course of 13 days as the salt was stepped up to 750°C and cooled back down. Ultra-High Purity (UHP) N_2 was the sparging gas used for the purification. The purification and salt transfer procedure were as follows:

- The purification vessel was loaded with the previously designated amounts of salt and Mg and was sealed. The vessel was then vacuumed to -30 inHg and refilled with UHP N_2 three times to remove the air within the vessel. UHP N_2 was continuously flushed through the vessel at 2.6 L/min (1.6 L/min sparging, 1 L/min overhead)
- The salt temperature was then stepped up to 750˚C over the course of 10 days with the major setpoints being 100˚C, 250˚C, 300˚C, and 600˚C. Exhaust products were monitored visually in the exhaust line and with mass spectrometer measurements. A pH probe in the exhaust jug measured the pH of the condensate collected from the purification. After the purification was completed the salt was frozen to set up for transfer.
- The purification vessel was connected to the tribology storage vessel with a transfer line. The storage vessel was similarly put under -30 inHg vacuum and flushed with UHP N_2 three times to remove air. This was done while the salt was frozen to prevent unintended salt transfer.
- The purification vessel and storage vessel were reheated to 550˚C and 75.7 kg of the purified salt was then moved through a ½" transfer line to a 316SS NPS 12" salt storage vessel. This was done by putting the storage vessel under -20 inHg vacuum and pressurizing the purification vessel to 5 psi, forcing salt up the dip tube, which sits 1½" off the bottom of the purification vessel to prevent transfer of particles that have settled to the bottom.
- The salt was transferred through a 10-micron filter system (double layer of 10-micron filter screen, 28 square inches of filter area) between the purification vessel and the storage vessel to remove any large particles that did not settle out of the salt during the purification.
- The salt was then brought to room temperature and frozen in the storage vessel until testing.
- Transferring the salt from the storage vessel to the tribology test bed vessel for testing followed the same procedure of heating both vessels to 550 ˚C, pulling vacuum on the tribology vessel, and pressurizing the storage vessel. No filter was used when transferring from the storage vessel to the tribology test bed.
- 69.9 kg of purified salt were transferred into the tribology test bed.

Tribology Test Bed Components

The tribology test bed is composed of a SS316 vessel and inner column assembly. The inner column assembly consists of a SS316 structure, shaft, three journal bearing housings, and a hub for holding pin samples. At 720˚C approximately 70 kg of salt is needed to submerge all pin and bearing samples while keeping the salt liquid level below ports of the vessel. Figure 1 shows the key components of the tribology test bed. Figure 2 shows a more detailed view of the inner column assembly. The 4.275 lb. loading weight applies a force to the middle bearing, which causes a deflection of the shaft and ensures contact between the three NiWC3b bearings and three NiWC3b-coated SS316 shaft sleeves.

Commented [a1]: It would be good to indicate the material of the different bearings.

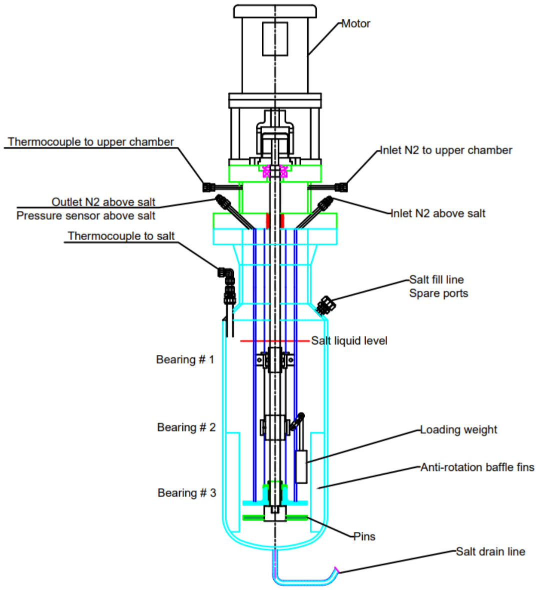

Figure 1. Tribology test bed components

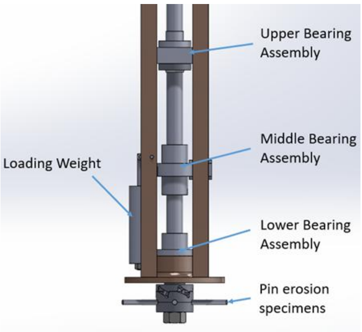

Figure 2. Inner column assembly

To reach the operating temperature of 720˚C the tribology rig vessel was heat traced and insulated as shown in figure 3. The neck region of the vessel was insulated with ¼" of Kaowool and ½" of Pyrogel. From the vessel flange and above, the tribology test bed is not insulated to keep motor and coupling components cool. The leads of the serpentine heaters are exposed for cooling because at high temperatures, formation of oxides on the surface of the leads can compromise the electrical contact. The heating is controlled by NI-DAQ PID control.

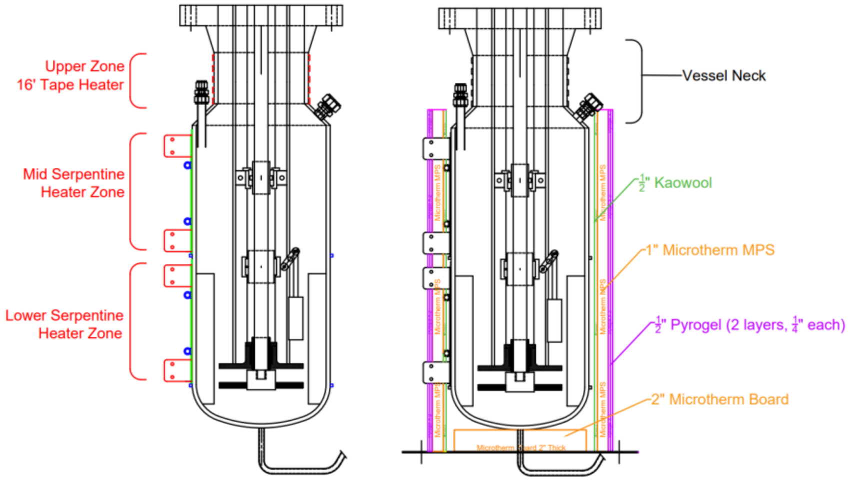

Figure 3. Tribology test bed heating zones (left) and insulation layers (right).

Experimental Procedure

The testing procedure for the tribology test bed included the following steps:

- **Pre-exposure measurements.** The pre-exposure measurements included measurements of the mass of the pins and bushings as well as dimensional measurements of the pins, bushings, and sleeves. Multiple measurements were taken and averaged, and a standard deviation was recorded for all measurements. Pre-exposure images of all samples were also taken for visual comparison.

- **Assembly of tribology test bed.** The inner column of the tribology test bed was assembled with the five pin specimens, three bearings, thee shaft sleeves, an unused shaft, unused fasteners, and thermal barrier consisting of four circular SS316 heat shields to reduce heat flow from the salt through the neck of the tribology vessel. After assembly, the inner column was lowered into the empty vessel of the tribology test bed and the flange was tightened.

- **Molten salt transfer.** The tribology test bed was heated to molten salt transfer temperature (550˚C) and 69.9 kg of salt was transferred from the storage vessel (also at 550˚C) into the tribology test bed. The salt level in the tribology rig was verified with a level detector to be above all bearing specimens and below all ports of the vessel and the motor was spun by hand to ensure free spinning.

- **Verification of speed conditions.** The tribology test bed was heated to a salt temperature of 720˚C and the motor was turned on to 700, 900, 1200, 1300, and 1400 RPM to check system vibration, motor amperage, and viscous heating for selecting the motor speed to be used for testing. The system was run at 1100 RPM due to viscous heat generation raising the salt temperature above 720˚C at higher speeds, which compromised the ability to control the salt temperature with the heater controls.

- **Molten salt run.** The motor of the tribology test bed was turned on to 1100 RPM and the heaters were set to maintain 720˚C throughout the test. Once the temperature and motor speeds were set, the test was run continuously for 500 hours. UHP N_2 was flushed through the test bed continuously during running. After 500 hours of runtime, the motor was turned off, the tribology test bed was cooled to 550˚C, and the salt was transferred back into the storage vessel through the salt drain line.

- **Disassembly.** Once the salt was drained, the system was cooled to room temperature over a few days. The motor was then removed and the inner column was pulled out of the reservoir to gain access to the samples and the bearings under test. The inner column of the test bed was then immersed in room-temperature distilled water overnight. The hub holding the pin samples was removed by cutting the nut securing it. The sleeve samples were removed by cutting the shaft in three locations, and then the bearing housings could be removed. Sonication of the pin hub and bearing housings at 50˚C allowed for removal of the pins and bearings. The pins, bearings and shaft sleeves were also sonicated to clean off residual salt.
- **Post exposure measurements & analysis.** The post-exposure measurements included measurements of the mass of the pins and bushings as well as dimensional measurements of the pins, bushings, and sleeves. Multiple measurements were taken and averaged, and a standard deviation was recorded for all measurements. Post exposure measurements were compared to pre-exposure measurements to determine dimensional and mass change. Post-exposure images of all samples were also taken for visual comparison.
- **Post exposure surface analysis.** Surface imaging of the pins and shaft sleeves was done with a white light optical profiler (Zygo 9000). Surface imaging of an unused control pin and shaft sleeve were taken for comparison of surface roughness to post-exposure samples.

Disassembly highlights

The stainless vessel and inner column structure were black in color but otherwise were in good condition. It was observed that the salt drained almost completely with a thin film of salt on horizontal surfaces. There was also some condensed vapor on the upper portion of the shaft above two of the thermal isolation sections. This layer was thin and didn't hinder any operation. The thermal isolation sections worked well; discoloration of the SS316 structure decreased significantly in the upper zones.

Figure 2. Internal structure before salt test.

Figure 5. Internal structure after salt test.

Figure 6. thermal isolation zones after salt test.

The bottom nut on the system that held the pin sample hub on the shaft had salt in the threads and it was required to cut this off to remove the pin samples. While removing the bottom hub one of the pin samples broke at the root where it was pinned into the hub. The rest of the samples were able to be removed with the hub. The hub was then sonicated in 50˚C distilled water. During sonication a second pin broke at the hub, but the remaining three pins survived. Upon inspection all the bearing surfaces looked to be in good condition. Sleeve surfaces were in good condition with an apparent mark on each sleeves circumference where contact was made with the corresponding bushing.

Figure 7. Pin specimen hub after removal from shaft. Pin samples are solid NiWC3B material

Figure 8. Upper shaft sleeve (~~solid~~ NiWC3B-coated SS316 material) after molten salt test.

Measurements

Dimensional measurements of the pins, sleeves, and bearings, shown in figure 9, were taken pre-exposure and post-exposure. All of the measurements were taken with a micrometer set with accuracy ranging from +-0.0001” to +-0.00024”. The measurements include diameter measurements of the pins at four radial locations and three axial locations. For the sleeves, diameter measurements were taken at two orthogonal locations and three axial locations. For the bearings, thickness measurements were taken at four radial locations and two axial locations (one axial location for the middle bushing). In addition to the thickness of the bushings, the inner diameter was measured at two orthogonal locations, with one being where contact was made between the bushing and the shaft sleeve. Once the post-exposure measurements were taken, they were compared to pre-test measurements to determine dimensional change from wear during the test. Some of the takeaways for each run are condensed in the following bullet points:

- NiWC3b pin specimens. Pin 4 was the only pin specimen that showed any decrease in diameter in any of its measurements. The average decrease of diameter on pin 4 was 0.00085 inches. The other four pins showed no measurable decrease in diameter due to erosive wear during the salt test. In fact, many of the dimensions measured a slight increase in diameter following the salt test.
- NiWC3b-coated sleeve specimens. No measurable decrease in diameter was found from the micrometer measurements of the sleeve specimens. Similar to the pin specimens, the upper and lower shaft sleeves measured a slight increase in diameter following the salt test.

- NiWC3b Bushings. Micrometer measurements show that wall thickness of the bushings changed minimally during the salt test. All bushings showed measurable change in their inner diameter measurements.

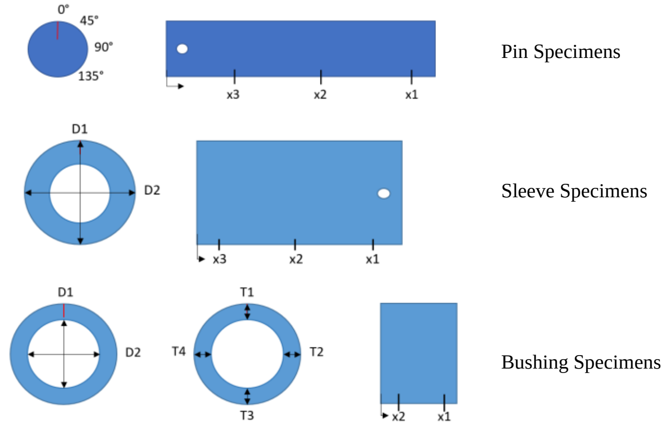

Figure 9. Diagram of dimensional measurement locations for pin, sleeve, and bearing specimens.

Surface Imaging

After the tribology test was complete, the pins, sleeves, and bushings were sonicated in DI water to clean off residual salt on their surfaces. The surface topography of the pin and sleeve samples were measured using a white light optical profiler (Zygo 9000) in order to identify wear the specimens experienced during the test.

Pin surface analysis

Surface imaging of the pins were taken at each of the twelve locations described previously for dimensional measurements. Figures 10 and 11 show surface imaging of pin 1 and the control pin respectively. The profiler showed a slight increase in surface roughness following the salt test, most likely due to MgO stuck to the surface of the pins exposed to salt. Table 2 gives the average surface roughness obtained for each pin from the surface analysis. No correlation between angle on the pin and surface roughness was seen.

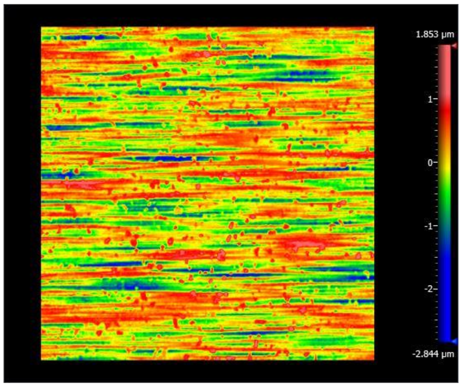

Figure 10. Surface imaging of pin 1 post salt test. Note the red spots of increased surface height present on pin 1 that are not present on the control pin are most likely MgO stuck to the surface from salt testing.

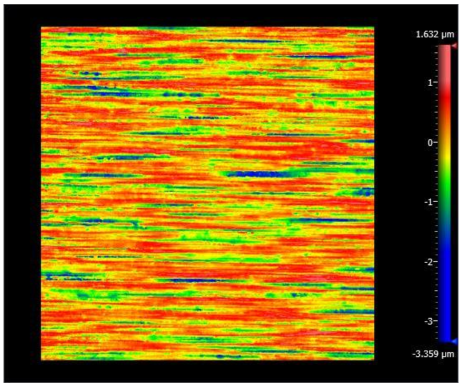

Figure 11. Surface imaging of control pin (not exposed to salt testing).

Table 2. Average surface roughness of pin samples.

Pin	1	2	3	4	5	Control
Roughness [µm]	0.5170	0.5858	0.5825	0.6359	0.6270	0.502

Sleeve surface analysis

Surface scans of sleeve specimens were taken along the length of each sleeve, as shown in figure 12. Four scans were taken from each sleeve at 90° spacings around the sleeve circumference. Figure 13 shows a scan taken for each sleeve where surface heights were averaged across a 1500-micron width of the scan. The plots show this average surface height along the length of the scan. The area of contact between the sleeve and its corresponding NiWC3b bushing is located between the two cursors on the plots.

Figure 12. Diagram of surface scans taken on sleeve specimens.

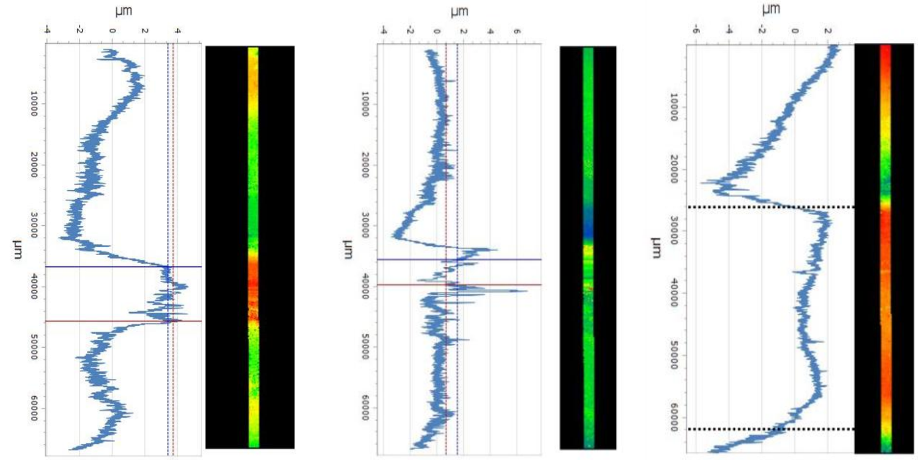
Upper sleeve

Middle sleeve

Lower sleeve

Figure 13. Surface scans of the three sleeve specimens (upper, middle, lower). Note that the are of contact with the bushing on each sleeve, shown as the area between the two cursors on each plot, is located in an area of elevated surface height relative to the rest of the sleeve.

The sleeve scans show the area of contact between the sleeve specimens and their corresponding bushings are in areas of elevated surface height relative to the rest of the shaft sleeve. To verify these results, measurements of the upper sleeve were taken with an Alicona optical profiler and a strip of the upper sleeve was coated with a 10 nm thickness of gold to increase reflectivity of the surface for more reliable measurements on the Zygo profiler. The Alicona measurements and Zygo measurements after gold-coating both confirmed the increased surface height at the area of contact.

One possible cause of the increased surface height in the contact area is material transfer from the NiWC3b bushings to the shaft sleeves. To look for material transfer from the bushings to the shaft sleeves, SEM imaging of the upper sleeve will be done to search for higher concentrations of nickel inside the contact area, which would suggest material transfer from the bushings.

Another possible cause of the increased surface height is corrosion of the shaft sleeve outside of the contact area. Figure 14 shows the three shaft sleeve specimens after being removed from the inner column assembly. From the images, it appears there may be some corrosion of the sleeves outside of the contact area while the contact areas themselves appear to be cleaner.

Upper sleeve Middle sleeve Lower sleeve

Figure 14. Shaft sleeves after removal from the inner column structure. There appears to be some corrosion outside of the contact areas and contact areas appear to be relatively clean.

Highlights and conclusions

- Micrometer~~Dimensional~~ measurements (accuracy of +-.00015”) made of~~–~~ the NiWC3b-coated~~B~~ sleeves and NiWC3b pins after 500 hours of testing in the ~~MgKCLNaCL~~ chloride salt (approximate composition: wt. 45.98% $MgCl_2$, wt. 38.91% KCl, and wt. 15.11% NaCl) indicated that there was no measurable ~~change~~decrease to the outside diameter, with the exception of pin sample 4. ~~don’t show significant wear of the test specimens.~~ Dimensional measurements of the bushings show small changes in the inner diameter following the salt test.
- Surface analysis of the pins showed a slight increase in surface roughness following the salt test and this is attributed to some evidence of ~~, most likely due to~~ MgO on ~~stuck to~~ the surface of the pins exposed to salt. No correlation between radial position (i.e., effect of salt velocity on the pin) was ~~observed indicating~~observed indicating no effect of surface erosion. ~~angle on the pin and surface roughness was seen.~~
- Surface analysis of the sleeves ~~show~~ revea~~i~~led a slight but measurable increase in surface height ~~increase in height~~ (corresponding to ~~slight increase in the diameter~~a slightly larger diameter) of the sleeve ~~the area of~~ at the contact area between the sleeve specimens and their corresponding bushings. T~~, The~~he ~~reason~~reason for an increase at this point is not known since it was expected that if anything there would be removal of material at this location. One possible explanation is that ~~are in areas of elevated surface height relative to the rest of the shaft sleeve. Possible reasons for the increased surface height are~~ material transfer from the NiWC3b bushings to the sleeve occurred resulting in slight thickness at this location. ~~and corrosion of the sleeves outside the area of contact.~~ More analysis needs to be done to determine the cause of this and the samples are being cross sectioned to allow~~y~~ a more detailed imaging with the SEM.
- Overall the test was very successful and ran without issue. The Cermet bearing material seemed to perform well over the 500 hours tests at 750C in the assumed wt. 45.98% $MgCl_2$, wt. 38.91% KCl, and wt. 15.11% NaCl ~~MgClKCLNaCL (put detailed composition)~~ chloride salt.

Commented [a2]: It would be good to specify the material of the sleeve and the bearings.

Commented [a3]: Try to be a little more formal and complete.

Commented [a4]: Ok but below we are saying that there is a dimensional change as determined by the surface scans. Maybe be more specific… micrometer measurements with an accuracy of xxx were unable to detect any dimensional changes … and then with the scans not the dimensional changes were found from an optical profilometer to be less than xxx (presumably much less than you could measure with the micrometer).

Formatted: Highlight

References

1. Zhao, Youyang & Klammer, Noah & Vidal, Judith. (2019). Purification strategy and effect of impurities on corrosivity of dehydrated carnallite for thermal solar applications. RSC Advances. 9. 41664-41671. 10.1039/C9RA09352D.